ACS APPLIED MATERIALS & INTERFACES

Research Article

www.acsami.org

Graphene Platform Used for Electrochemically Discriminating DNA Triplex

Lingyan Feng, Zhijun Zhang, Jinsong Ren, and Xiaogang Qu*

Laboratory of Chemical Biology, Division of Biological Inorganic Chemistry, State Key Laboratory of Rare Earth Resource Utilization, Changchun Institute of Applied Chemistry, University of Chinese Academy of Sciences, Chinese Academy of Sciences, Changchun, 130022, China

Supporting Information

ABSTRACT: Triplex DNA has received great attention as new molecular biology tools and therapeutic agents due to their possible novel functions in biology systems. Therefore, it is important to distinguish triplex from among different forms of DNA, such as single-stranded and double-stranded DNA. In this report, several electrochemical techniques, cyclic voltammetry, electrochemical impedance spectroscopy, different pulse voltammetry, and electrochemiluminescence were used for distinguishing this unique structure among different DNA formations by using functionalized graphene/Nafion–$Ru(bpy)_3^{2+}$ (bpy = 2, 2′-bipyridine) modified glass carbon electrode. The different interactions between nucleotides and graphene surface and $Ru(bpy)_3^{2+}$ mediated guanine oxidation produced quite different electrochemical responses. Guanine bases are hidden inside the folded triplex DNAs, which are much less susceptible to be oxidized by $Ru(bpy)_3^{3+}$ produced on electrodes. Furthermore, the effect of guanine bases stacking in triplex also influences the electrochemical behaviors. By changing the different position and distance of guanine bases in DNA sequences, we found that the conjoint way of several guanines strongly influenced the catalytic electrochemical responses on graphene surface. Our results provide new insight into determination of less stable protonated triplex formation by using graphene-based rapid, low-cost and sensitive electrochemical techniques.

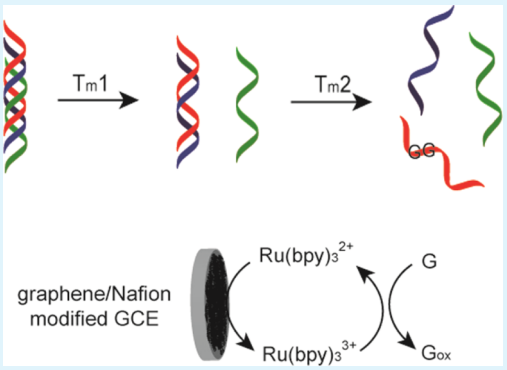

KEYWORDS: *Graphene, triplex, guanine, electrochemistry, stacking base*

1. INTRODUCTION

Graphene is a promising transducing platform for biosensor design, which was reported to have an elusive two-dimensional (2D) structure with numerous unexpected electrical properties.[1−3] Graphene-based DNA biodevices, such as DNA carriers,[4] graphene nanopores for DNA sequencing,[5] and graphene-DNA biosensors[6] have been highlighted with highly sensitivity, efficiency, and excellent biostability. Through different hydrophobic, electrostatic or hydrogen bonding interactions, DNA molecules with multiple primary amines can adsorb with the carboxylic and phenolic groups on graphene surfaces.[7,8] Among the four nucleotides, guanine shows the strongest interaction with graphene surface, which is similar to the interaction with single-walled carbon nanotubes.[9−11] A number of electrochemical works have been reported about DNA behavior on graphene modified electrode. They are frequently relied on the use of the electrochemical properties of single base[12,13] or the use of the interaction between single stranded DNA (ssDNA) adsorbed on graphene surface being stronger than duplex (dsDNA) or quadruplex structures.[14] Very recently, the different DNA structures have been examined on the graphene modified electrode surface, and the electrochemical surface is sensitive enough to detect single nucleotide polymorphism.[15,16] However, until now, there is little discussion in the literature of the electrochemical response of one unique DNA structure, the triplex helix, on graphene surface, and research on the catalytic behavior between triplex DNA and a graphene/Nafion–$Ru(bpy)_3^{2+}$ modified substrate is also yet to be developed.

Because of the potential applications of the nucleic acid triplex in the biomedical field, it has recently received great attention with the third strand binding as an artificial routine to inhibit gene expression selectively or reagents delivery to special genomes.[17] It usually forms through a third pyrimidine strand binding to duplex major groove, which is usually paralleled with Hoogsteen base pairing.[18,19] For most triplex DNAs, the third strand association is considerably less stable than the duplex.[20] The corresponding N3 positions of cytosines of the third strand are always protonated with a pK_a value of around 4.5 to form CGC^+ triplets, and the whole triplex structure can be stabilized by favorable electrostatic effects. Under acid or near physical conditions, the triplets TAT and CGC^+ are usually well formed, with the electroactive guanine buried into the hydrophobic environment.[21,22]

Received: December 10, 2013
Accepted: February 5, 2014
Published: February 5, 2014

   dx.doi.org/10.1021/am405676n | ACS Appl. Mater. Interfaces 2014, 6, 3513−3519

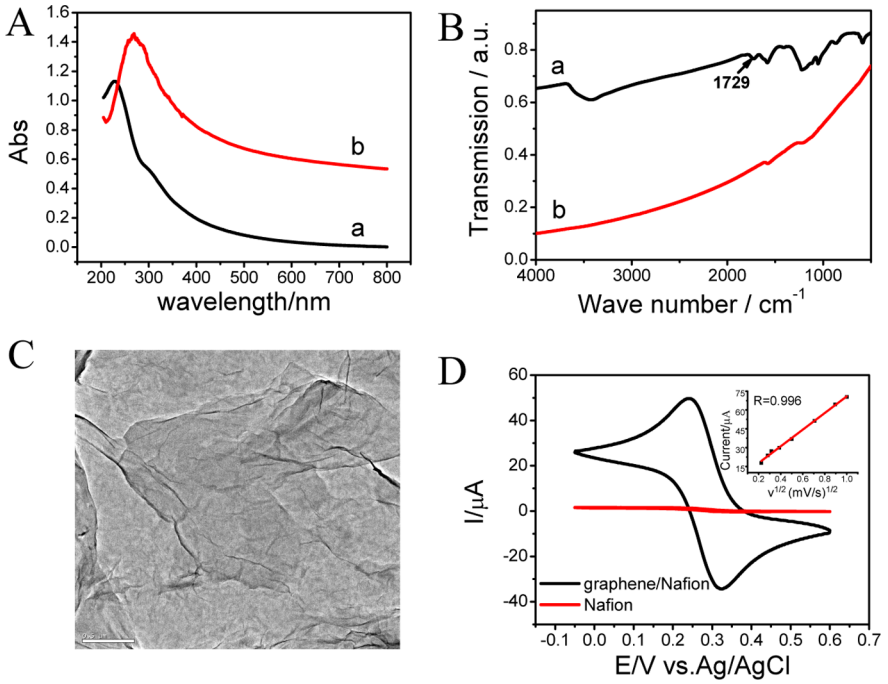

Figure 1. Characterizations of graphene materials and modified electrodes. (A) UV−Vis and (B) FR-IR spectrogram of (a) GO and (b) graphene. (C) TEM image of graphene layer (scale bar = 500 nm). (D) CVs of graphene/Nafion modified GCE and only Nafion modified GCE (scan rate = 10 mV/s).

Some spectral methods, such as UV−Vis, circular dichroism, and capillary electrophoresis, etc. have been widely used to distinguish DNA strands in different forms.[18−23] However, they usually need larger samples and higher concentrations. For other methods, such as NMR,[24] X-ray diffraction (XRD),[25] mass spectra (MS),[26] etc. it needs expensive instrument, special training to operate, or the high quality crystal sample preparation for measurements, which are also time consuming and have high costs. In addition, traditional gel migration and DNase I footprinting has the hazard of toxicity or radiation.[23] Compared to them, the electrochemical technique is much easier to manipulate, low-cost, and suitable for filed analysis.[20,27,28] It has been considered as a highly sensitive and effective technique for DNA structure change detection and nucleic acid with redox-active molecule (such as daunomycin, methylene blue, etc.) interactions.[29−31] We have used cyclic voltammetry (CV) and differential pulse voltammetry (DPV) means to detect the less stable triplex formation using one anticancer molecular coralyne as a probe, and it proved that the less stable triplex structures can be distinguished by using sensitive electrochemical techniques.[20]

In this report, we found that the triplex helix was easily distinguished among different ssDNA and dsDNA by using sensitive electrochemical techniques with functionalized graphene/Nafion−$Ru(bpy)_3^{2+}$ modified electrodes. Especially, electrochemical impedance spectroscopy (EIS) is reported as sensitive enough to measure the surface changes of different electrodes,[32,33] allowing label-free determination of triplex DNA. Different formed DNA also shows quite distinguishable DPV and electrochemiluminescence (ECL) responses under different pH. For triplex DNA, guanine is hidden inside it with a less susceptible state to be oxidized by $Ru(bpy)_3^{3+}$ produced on electrode. The signal of triplex DNA decreased compared to its corresponding duplex and single strands. Furthermore, by changing the different position and distance of guanine bases in DNA sequences, we found that the conjoint way of several guanines strongly influenced the catalytic electrochemical responses on the graphene surface.

2. EXPERIMENTAL SECTION

Reagents. Graphite was purchased from Sinopharm Chemical Reagent Co. Ltd (Shanghai, China). Tris(2,2′-bipyridyl) ruthenium(II) chloride hexahydrate ($Ru(bpy)_3Cl_2$) was purchased from Sigma. DNA sequences were synthesized by Sangon (Shanghai, China). Solutions were all prepared in ultrapure water purified through a Mill-Q system (Millipore, USA).

Preparation of Graphene. Graphene oxide (GO) was firstly obtained from graphite according to the Hummer's method. Graphene was synthesized as follows: 2.5 mL of GO solution (1 mg/mL), 2 μL of hydrazine solution (85 wt % in water), and 40 μL of ammonia solution (25 wt % in water) were mixed in a total volume of 10 mL. The mixture was put into a water bath (95 °C) for 1 h. Prepared graphene dispersions were used for further characterization and modified electrode fabrication.

Preparation of Graphene/Nafion and Graphene/Nafion−$Ru(bpy)_3^{2+}$ Modified GCE. The glass carbon electrode (GCE, Φ = 3.0 mm) was pretreated. A 90 μL graphene solution (250 μg/mL) and 10 μL of 0.5% Nafion solution were mixed to give a homogeneous solution. Then we dropped 5 μL of mixture on the clean GCE surface and dried it under vacuum at room temperature. The modified GCE with graphene/Nafion composite film was incubated in a $Ru(bpy)_3^{2+}$solution (1 mM) for 30 min to adsorb $Ru(bpy)_3^{2+}$ and then the surfaces were washed with water to remove the physical adsorbed $Ru(bpy)_3^{2+}$ on the surface.

Instruments and Measurements. Each DNA strand was diffused in phosphate buffer with a stock solution before use. Triplex DNA and duplex DNA were prepared by mixing euquimolar amounts of appropriate strands in corresponding buffers, which were heated to 90 °C and cooled to room temperature slowly. DNA UV melting curves were measured on a JASCO V-550 UV/Vis spectrophotometer with a Peltier temperature control accessory. Circular dichroism (CD) results were carried out on a Jasco J-810 spectropolarimeter. The CD optical chamber was deoxygenated using dry purified nitrogen (99.99%, 45 min) before measurements and the nitrogen atmosphere was kept

during the scanning. Three times were collected and automatically averaged. FT-IR characterization was measured on a BRUKE Vertex 70 FT-IR spectrometer. Mass spectral measurements were carried out with the negative-ion mode on a Thermo LTQ XL ion trap mass spectrometer (Thermo, San Jose, CA, USA). The sample flow rate is 5 mL/min via a Harvard syringe pump (Holliston, MA, USA), with needle voltage of 3.5 kV, capillary voltage −20 V, and tube lens offset −190 V.

Electrochemical measurements were measured with the CHI 660B (CH Instruments, Inc., Austin, TX). The working electrode was a glass carbon electrode (GCE), the reference electrode was an Ag/AgCl (3 M KCl), and platinum wire acted as the counter electrode. EIS was performed at 0.24 V (vs Ag/AgCl) (10 mM PBS, 10 mM 1:1 $K_3[Fe(CN)_6]/K_4[Fe(CN)_6]$ solution, 0.5M NaCl). The impedance frequency range was 10^{-2}−10^5 Hz. The amplitude of the applied sine wave potential was set to 5 mV. Cyclic potential sweep experiments were scanned in from 0.2 to 1.3 V and then returned to 0.2 V (10 mM PBS, 500 mM NaCl, 50 μM $Ru(bpy)_3^{2+}$), and ECL signals versus time were recorded by the BPCL-2-TGC Ultra Weak Luminescence Analyzer (Beijing, China). Differential pulse voltammogram (DPV) signals were carried with the potential interval of 0.2 to 1.3 V (vs Ag/AgCl), and the conditions were as follows: modulation amplitude 0.05 V, step potential 0.001 V, scan rate 0.004 V/s (10 mM PBS, 500 mM NaCl, 50 μM $Ru(bpy)_3^{2+}$). Unless otherwise specified, the DNA used for measurements were 2 and 5 μM for electrochemical characterizations of 20 μL volumes of T1G, T2G, and T3G triplexes.

3. RESULTS AND DISCUSSION

Preparation and Characterization of Graphene Materials. Graphene was obtained through the Hummer's method and then reduced by hydrazine.[34] UV absorption and FT-IR spectrum confirmed graphene formation (Figure 1A,B), the absorption of graphene oxide (GO) solution red-shifted from 231 to 270 nm gradually. The absorption band at around 1700 cm^{-1} was attributed to the carboxyl group in the FT-IR spectra.[27,33] A transmission electron microscopy (TEM) image demonstrated the graphene dispersed well with a thin wrinkling paperlike structure (Figure 1C). A graphene/Nafion modified glass carbon electrode (GCE) surface was first constructed. It showed an extraordinary electron transfer property, as seen in the CVs, compared with only Nafion modified electrode, and underwent a diffusion process (Figure 1D and inset).[20,33] The modified electrode was stable enough even scanned hundreds of rounds (Supporting Information, Figure S1).

Oligonucleotide Characterization. A triplex usually forms through an oligopyrimidine strand binding to the duplex major groove in a sequence-specific manner through Hoogsteen base pairing.[17−20] Here, a 21-mer triplex containing CGC and TAT triplets (T1, all DNA sequences used are shown in Table 1) was first employed as a model DNA. The formation of T1 was significantly pH and salt-dependent in solution, as summarized in Table 2. There were two well resolved transitions in triplex melting profiles under near physiological conditions: the first T_m1 transition at low temperature was ascribed to the third strand dissociated from corresponding duplex strand, whereas the second T_m2 transition was due to the Watson−Crick helix denaturation[18,20] (Figure 2A). Under basic pH, the triplex strand was not formed and there was only the double-to-coil transition. Under room temperature (25 °C) and optimized salt concentration (500 mM NaCl), DNA was mainly in triplex at pH 4.5 with T_m1 and T_m2 cooperative, and at pH 6.0, it was in the equilibrium state between duplex and triplex structures. When the solution pH was increased to 6.5, most DNA was in duplex, and no triplex was observed at pH 7.2. The formation of T1 DNA was further confirmed by its CD characteristic curve with the presence of negative bands around 210 nm, which is recognized as an indicator signal of triplex formation (Supporting Information, Figure S2).[18,19]

Table 1. Sequences of the Oligomers Used in This Study

oligo strands	sequences
triplex 1 (T1)	5′-GAG AGG AGA GAG AAG AGG AAG-3′
	3′-CTC TCC TCT CTC TTC TCC TTC-5′
	5′-CTT CCT CTT CTC TCT CCT CTC-3′
mt31	5′-AGA GAA GTT TTC TTC TCT TTT TTT TCT CTT C-3′
mu31	5′-TCT TAT CTT CGT TAT TAC TAT TCT GTT CTG T-3′
T1G	5′-TTCTCTCTCTCTCT-3′
	3′-AAGAGAGAGAGAGA-5′
	5′-TTCTCTCTCTCTCT-3′
T2G	5′-TTCCTTCCTTCCTT-3′
	3′-AAGGAAGGAAGGAA-5′
	5′-TTCCTTCCTTCCTT-3′
T3G	5′-TTCCCTTTTCCCTT-3′
	3′-AAGGGAAAAGGGAA-5′
	5′-TTCCCTTTTCCCTT-3′

Table 2. Melting Temperatures of 2 μM T1 DNA Obtained from the First Derivative Curves of Their Corresponding Melting Curves under Different Buffer Conditions

Na^+(mM)/T_m/pH		4.5	6.0	6.5	7.2
200	T_m1	62.4	26.5	16.7	64.8
	T_m2		63.9	64.5	
500	T_m1	67.1	28.1	20.4	69.1
	T_m2		65.2	67.5	
800	T_m1	65.1	34.8	22.8	71
	T_m2		70.3	71.2	

Impedance Measurements of Inter- and Intramolecular Triplex. The different forms of DNA, ssDNA, duplex, and triplex have quite different interactions between nucleotides with a graphene surface. ssDNA adsorbs on the graphene platform through π−π interactions, whereas duplex and triplex mainly bind to graphene via DNA end electrostatic/hydrogen bonding interactions.[7−11] First, the EIS technique was used to study the different forms of DNA. As shown in Figure 2B, the R_{et} value of graphene/Nafion modified electrode was only 17.8 ± 1.3 Ω. It significantly increased after the DNA strands immobilization onto the surface. The R_{et} value was 36.9 ± 0.9 Ω for T1 DNA, and they were 44.2 ± 2.1 Ω and 58.1 ± 1.6 Ω for duplex and ssDNA, respectively. The different R_{et} were attributed to the different DNA hindrance effects on the $[Fe(CN)_6]^{3-/4-}$electron transfer process. The negatively charged DNA phosphate backbone would repel the negatively charged redox probe, thus increasing the R_{et} values.[27] Because equal molar of DNA nucleotides of different DNA structures were used on the graphene surface, the random ssDNA would bind strongly on the graphene surface, which resulted in higher impedance and stronger hindrance on the electron transfer. To further confirm this, one 31-mer mt31 DNA, which can form an intramolecular triplex structure containing TAT and CGC triplets, was also subjected to EIS measurement and compared with another 31-mer mu31 DNA, which was designed not to form the intramolecular triplex while containing the same nucleotides of mt31 with a scrambled sequence (Table 1).[35] The mt31 DNA could form mainly a triplex structure in a pH 5.5 solution and duplex in a pH 7.5 buffer (Figure 2C),

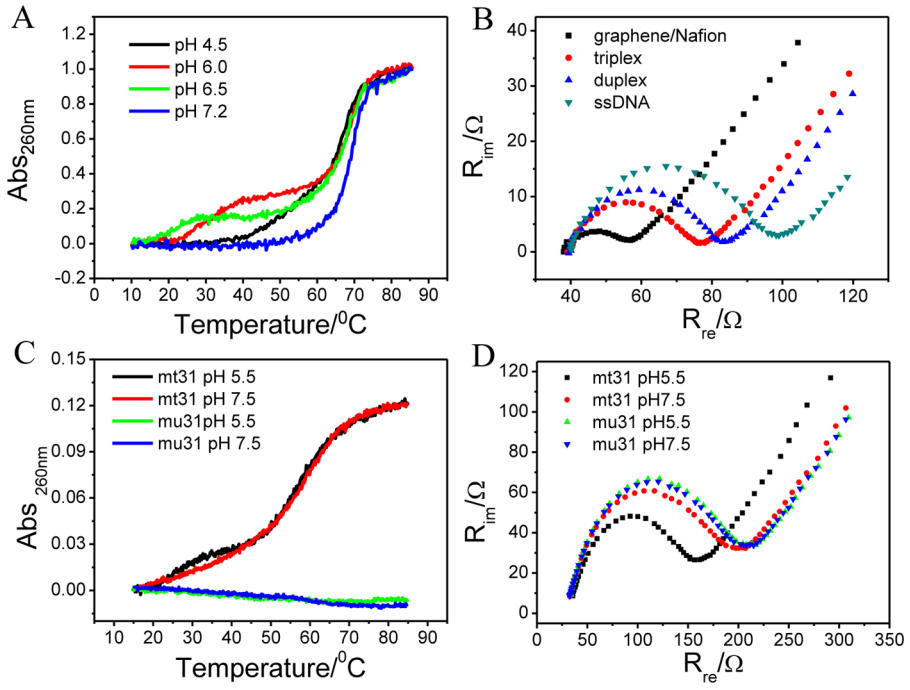

Figure 2. Spectra and EIS of inter- and intramolecular triplex. (A) UV melting of 2 μM T1 DNA in 10 mM PBS containing 500 mM NaCl with different pH values (B) EIS of 2 μM T1 DNA in triplex, duplex, and ssDNA forms on graphene/Nafion modified GCE. (C) UV melting of 31-mer mt31 and mu31 DNA in different pH buffers. (D) EIS of 2 μM mt31 and mu31 DNA in different pH buffers adsorbed on graphene/Nafion modified GCE.

respectively, whereas mu31 DNA was a random strand without any structure under the same experimental conditions (Figure 2C). The corresponding EIS measurements showed that the changed R_{et} value for mt31 was 41.8 Ω between triplex and duplex forms, indicating DNA structural transition under different pH conditions (Figure 2D). For mu31, the R_{et} value was almost unchanged (Figure 2D). This indicated that mu31 DNA was random sequence and did not form a structure under different pHs.

CV and DPV Measurements. A graphene/Nafion–$Ru(bpy)_3^{2+}$ modified platform was further constructed to distinguish the triplex structure. Nafion, as a classic cation-exchange polymer, was useful for $Ru(bpy)_3^{2+}$ immobilization with selective high ion-exchange and stable electrochemical property.[36] Figure S3A showed the CVs of graphene/Nafion–$Ru(bpy)_3^{2+}$ modified electrode with different scan rates. It appears a redox pair attributed to $Ru(bpy)_3^{2+}/Ru(bpy)_3^{3+}$ electroactive pair. The anodic peak current was proportional to the square root of the scan rate, indicating that the immobilized $Ru(bpy)_3^{2+}$ underwent a diffusion progress, which was consistent with previous report (Supporting Information, Figure S3B).[20]

Among the four nucleotides, guanine was the most electroactive base among different DNA bases and gave an irreversible peak around ~+1.00 V (vs Ag/AgCl). $Ru(bpy)_3^{2+}$, as a mediator, could be employed to gain the amplified signal for DNA detection[37,38] based on the electrocatalytic mechanism (Scheme 1). With nuclei acids present, the metal complex catalysed the guanine oxidation as the cycle below:

$$Ru(bpy)_3^{2+} \rightarrow Ru(bpy)_3^{3+} + e^- \quad (1)$$

$$Ru(bpy)_3^{3+} + DNA \rightarrow Ru(bpy)_3^{2+} + DNA_{ox} \quad (2)$$

Scheme 1. Schematic Representation of Triplex DNA Dissociation into Different Forms and the Electrochemical Catalytic Cycle between $Ru(bpy)_3^{3+/2+}$ and Guanine Base

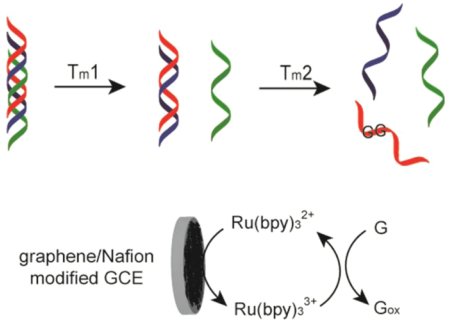

where DNA_{ox} contained guanine oxidized by a single electron. The enhancements in the oxidation current for $Ru(bpy)_3^{2+}$ with DNA strands were due to catalytic cycling of $Ru(bpy)_3^{3+/2+}$.[38]

Compared to duplex and ssDNA, the guanine bases were buried inside the triplex DNA structure, which would increase the distance with graphene/Nafion–$Ru(bpy)_3^{2+}$ modified electrode, then decreased the catalytic currents observed from the reaction of $Ru(bpy)_3^{3+}$ with guanine.[39−41] CVs of T1 DNA were performed in different pH buffers containing 50 μM $Ru(bpy)_3^{2+}$ (Figure 3A). As predicted, the catalytic current of CV increased as the pH increased. Furthermore, DPV measurement was also conducted under the same experimental conditions. As a pulse technique, DPV allows much higher sensitivity than other sweep methods, even with very low concentrations of a redox probe.[20] By eliminating the capacitive charging current, only Faradaic current on the electrode can be measured in DPV curves.[42] The DPV peak occurred at 1.08 V (vs Ag/AgCl), and the current also increased obviously as the pH increased (Figure 3B). At pH 4.5, T1 DNA formed a triplex

dx.doi.org/10.1021/am405676n | ACS Appl. Mater. Interfaces 2014, 6, 3513−3519

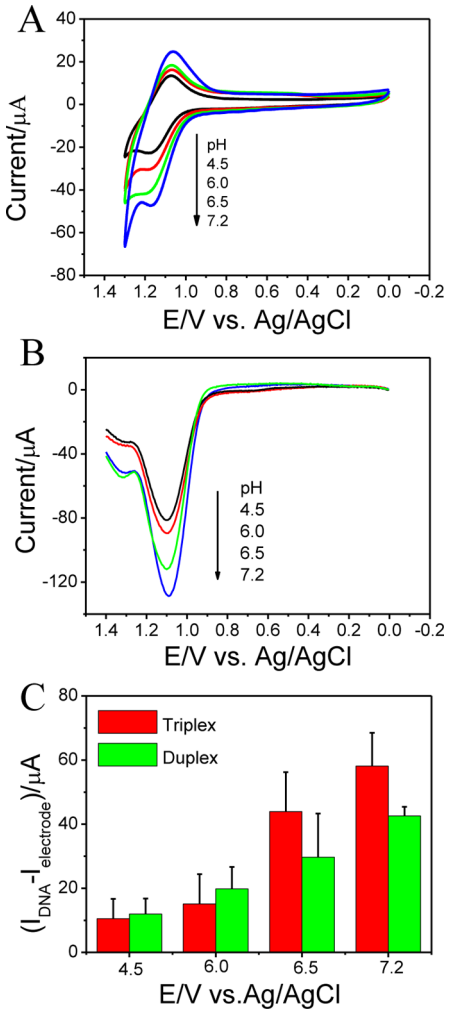

Figure 3. Electrochemical results of T1 triplex DNA. (A) CVs and (B) DPVs of 2 μM T1 DNA in 10 mM PBS containing 500 mM NaCl with different pH values. (C) Comparison of DPV values of triplex and duplex DNA under different pH conditions.

with guanine folded into the triplex formation (Figure 2A), and the catalytic current was hardly observed. As the solution pH value was further increased, the DNA strand unfolded, and the catalysis occurred due to guanine oxidation process. Triplex could be distinguished through the electrocatalytic reactivity between $Ru(bpy)_3^{3+}$ and guanine.[39−41] The results of CV and DPV measurements were consistent, and the latter method was more effective (Figure 3A,B). Because the electron transfer of $Ru(bpy)_3^{3+/2+}$ proceeded via a proton-coupled pathway,[39−41,43] we carefully compared DPV currents of triplex and duplex formations under the same pH conditions (Supporting Information, Figure S4). The relative DPV current changes ΔI ($I_{DNA} - I_{electrode}$) of duplex and triplex are shown in Figure 3C after subtracting the background current of the modified electrode. It increased dramatically for triplex helices compared to duplex, especially from pH 6.0 to pH 6.5, which corresponds to the triplex−duplex transition. The result further indicated that DNA structural transitions could result in current signal changes. In addition, the DPV results of T1 DNA appear to have a little peak around 0.67 V (vs Ag/AgCl) after three scanning rounds (Supporting Information, Figure S5 and its inset). It might be attributed to the oxidation of 8-oxoG, which formation in the DNA moiety is considered the most commonly measured product of DNA oxidation. But further work still need to be developed for more exact information.[44,45]

Electrochemiluminescence Measurements. Electrochemiluminescence (ECL) is chemiluminescence triggered by an electrochemical technique; it has received considerable attention because of its simplicity and versatility.[46,47] Among all systems of ECL methods, $Ru(bpy)_3^{2+}$-based ECL has development and abundant analytical applications, especially in the determination of a number of biologically important species and constructing related biosensors.[48,49] $Ru(bpy)_3^{2+}$ generated ECL through reacting with guanine bases and a stronger electrochemical signal could be provided from single strand according to the following pathway:

$$Ru(bpy)_3^{2+} \rightarrow Ru(bpy)_3^{3+} + e^- \quad (1)$$

$$Ru(bpy)_3^{3+} + G \rightarrow Ru(bpy)_3^{2+} + G^* + H^+ \quad (2)$$

$$G^* + Ru(bpy)_3^{3+} \rightarrow G_{2ox} + Ru(bpy)_3^{2+*} \quad (3)$$

$$Ru(bpy)_3^{2+} \rightarrow Ru(bpy)_3^{3+} + h\nu \quad (4)$$

The $Ru(bpy)_3^{2+}$ can be firstly oxidized on surface (eq 1) and a guanine base is then oxidized into a guanine radical (eq 2), which can continue reacting with $Ru(bpy)_3^{3+}$ to produce a doubly oxidized guanine (G_{2ox}) and excited $Ru(bpy)_3^{2+*}$ sites (eq 3). Finally, the excited $Ru(bpy)_3^{2+*}$ will emit light while decaying back to the ground-state products (eq 4).[38,50] No sacrificial reductant is required. The ECL reaction is directly initiated by electrochemical catalytic oxidation of guanines in DNA as reported by Thorp et al.[50] Here, we compared the DPV and corresponding ECL behaviors of different DNA forms (Figure 4). The ECL signal was recorded when corresponding CV was scanning, and it increased in the

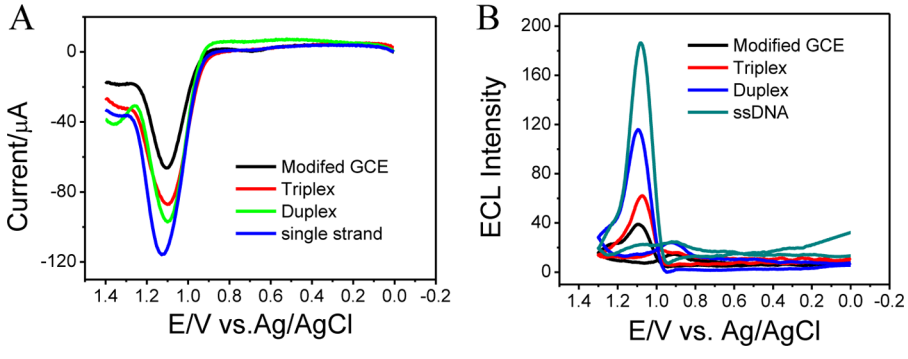

Figure 4. (A) ECLs and (B) DPVs of different structures of DNA on graphene/Nafion−$Ru(bpy)_3^{2+}$ modified GCE.

dx.doi.org/10.1021/am405676n | ACS Appl. Mater. Interfaces 2014, 6, 3513−3519

presence of DNA. The luminescence outset appeared near 0.92 V and the maximum ECL signal was slightly positive of DPV at 1.09 V vs. Ag/AgCl. The optimal scan rate for ECL was 20 mV/s (Figure S6). Both of the DPV and ECL results showed that triplex had the least sensitive electrochemical signals, which were quite different from its corresponding dsDNA and ssDNA. The enhanced DPV and ECL signals were observed for ssDNA, in which guanine was more exposed outside. The triplex formation inhibited access of electrogenerated $Ru(bpy)_3^{3+}$ to the buried guanine, and the protonated cytosines would probably draw the density of electron by forming hydrogen bond between guanine and cytosine, which will result in a less electron-rich guanine that made more difficult to be oxidized.[39−41] The charge transport through triplex formation would not be affected largely as shown previously, but the trapping of radical cation would be inhibited.[40] On the basis of these two reasons reducing electron transfer rates between guanines and $Ru(bpy)_3^{3+/2+}$ complex, the observed electrochemical signals appeared much lower.

Conjoint Way of Guanines Effects. We also designed triplex strands with six isolated guanines (T1G), three GG doublets (T2G), or two GGG triplets (T3G) (DNA sequences are shown in Table 1). These triplexes could then be used with the exactly same concentration of DNA strand and absolute guanine concentration. All three DNAs could form triplex structures confirmed by UV melting curves (Figure 5A) and MS spectra of triplex (Supporting Information, Figure S7). To avoid the influence of triplex dissociation under experimental conditions and consider the solely factor of guanine multiplets, the following measurements were all carried out under controlled temperature condition at 15 °C. The DPVs and ECLs of $Ru(bpy)_3^{2+}$ with three triplex strands are shown in Figure 5B,C. The conjugated guanine multipletes clearly resulted in enhanced electrochemical reactivity in triplex DNA. According to the ECL intensity, T3G and T2G were enhanced by a factor of 6.6 and 4.7 compared to T1G with isolated guanines, respectively, which were more sensitive than DPV results of 4.1 and 2.9. In the process of DNA mediating electron transfer, GG doublets were usually considered as a "hole trap", which cleavage was usually determined by a remote acceptor oxidation to get the relative rates of electron transfer.[51] However, until now, there was no report of comparing the effect of base stacking on redox active guanine using more sensitive electrochemical DPV and ECL techniques, although the selective oxidation of guanine base has been well-reported with sequencing gels.[38] By a comparison of the enhanced ratio of GG doublets to single guanines, both of the above electrochemical results were more sensitive than that observed by sequencing gels, which gave a ratio of 1.8,[50] while being similar to the result of 3−5 reported by Schuster et al.[52] In the GGG triplets, the middle G was generally more reactive.[39−41,52] For each stacked guanine, the enhancement degree would be quite different, and the enhancement factors of DPV and ECL for triplex DNA were comparable with the previous result obtained from the apparent rate constant in CV measurement of single strand DNA.[50] The conjoint way of several guanine bases clearly influenced the electrochemical response of triplex DNA on graphene/Nafion−$Ru(bpy)_3^{2+}$ modified electrode, and the adjacent guanines of T3G gave the most enhanced reactivity compared to the GG doublets and isolated guanines.

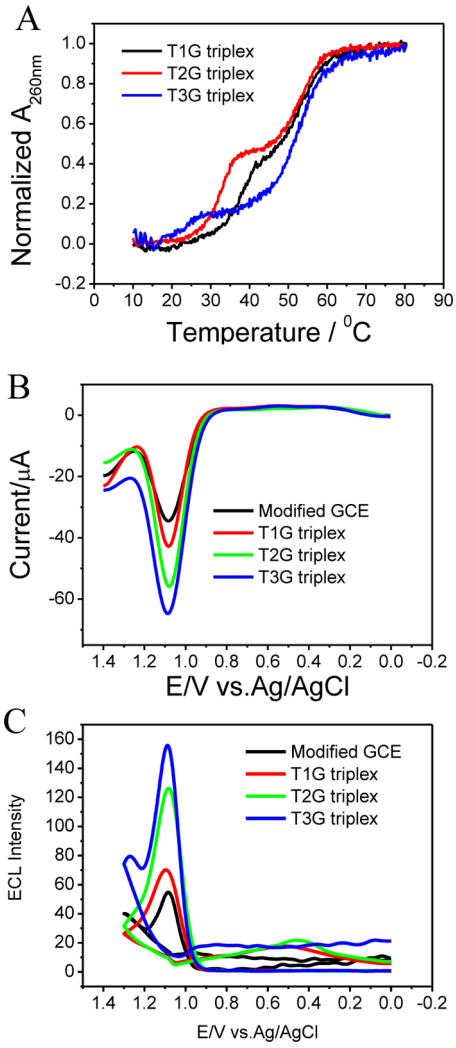

Figure 5. Conjoint way of guanines effects in triplex. (A) UV melting of 1 μM T1G, T2G, and T3G triplex DNA. (B) DPVs and (C) ECLs of 5 μM T1G, T2G, and T3G triplex on graphene/Nafion−$Ru(bpy)_3^{2+}$ modified GCE (300 mM NaCl solution).

4. CONCLUSIONS

In summary, the graphene/Nafion and graphene/Nafion−$Ru(bpy)_3^{2+}$ modified electrodes are successfully constructed for distinguishing triplex DNA among different ssDNA and dsDNA. Several electrochemical techniques, such as CV, EIS, DPV, and ECL, are used and compared in our studies. Furthermore, the effect of guanine bases stacked in triplexes also influences the electrochemical behaviors. In a comparison of the different position and distance of guanine bases in DNA sequences, the results clearly indicate that the conjoint way of several guanines strongly affect the catalytic electrochemical responses on graphene surface. Our work will shed light on determination of less stable protonated triplex formation by using graphene-based rapid, low-cost, and sensitive electrochemical techniques.

■ ASSOCIATED CONTENT

Supporting Information

Stability of graphene/Nafion electrode, CVs of graphene/Nafion−$Ru(bpy)_3^{2+}$ modified electrode with different scan rates, CVs and DPVs of D1 DNA, and optimal scan rate of ECL

measurements. This material is available free of charge via the Internet at http://pubs.acs.org.

AUTHOR INFORMATION

Corresponding Author

*X. Qu. E-mail: xqu@ciac.ac.cn. Tel./Fax: +86 431 85262656.

Notes

The authors declare no competing financial interest.

ACKNOWLEDGMENTS

This work was supported by 973 Project (2011CB936004, 2012CB720602), and NSFC (21210002, 91213302).

REFERENCES

(1) Pumera, M. *Chem. Soc. Rev.* **2010**, *39*, 4146−4157.
(2) Song, Y.; Wei, W.; Qu, X. *Adv. Mater.* **2011**, *23*, 4215−4236.
(3) Li, X.; Zhang, G.; Bai, X.; Sun, X.; Wang, X.; Wang, E. *Nat. Nanotechnol.* **2008**, *3*, 538−542.
(4) Wang, Y.; Li, Z.; Hu, D.; Lin, C. T.; Li, J.; Lin, Y. *J. Am. Chem. Soc.* **2010**, *132*, 9274−9276.
(5) Schneider, G. F.; Kowalczyk, S. W.; Calado, V. E.; Pandraud, G.; Zandbergen, H. W.; Vandersypen, L. M. K.; Dekker, C. *Nano Lett.* **2010**, *10*, 3163−3167.
(6) Stine, R.; Robinson, J. T.; Sheehan, P. E.; Tamanaha, C. R. *Adv. Mater.* **2010**, *22*, 5297−5300.
(7) Patil, A. J.; Vickery, J. L.; Scott, T. B.; Mann, S. *Adv. Mater.* **2009**, *21*, 3159−3164.
(8) Varghese, N.; Mogera, U.; Govindaraj, A.; Das, A.; Maiti, P. K.; Sood, A. K.; Rao, C. N. R. *ChemPhysChem.* **2009**, *10*, 206−210.
(9) Gowtham, S.; Scheicher, R. H.; Ahuja, R.; Pandey, R.; Karna, S. P. *Phy. Rev. B* **2007**, *76*, 033401.
(10) Zheng, M.; Semke, E. D. *J. Am. Chem. Soc.* **2007**, *129*, 6084−6085.
(11) Li, X.; Peng, Y.; Qu, X. G. *Nucleic Acids Res.* **2006**, *34*, 3670−3676.
(12) Zhou, M.; Zhai, Y.; Dong, S. *Anal. Chem.* **2009**, *81*, 5603−5613.
(13) Yin, H.; Zhou, Y.; Ma, Q.; Ai, S.; Ju, P.; Zhu, L.; Lu, L. *Process Biochem. (Oxford, U. K.)* **2010**, *45*, 1707−1712.
(14) Li, D.; Song, S.; Fan, C. *Acc. Chem. Res.* **2010**, *43*, 631−641.
(15) Bonanni, A.; Pumera, M. *ACS Nano* **2011**, *5*, 2356−2361.
(16) Bonanni, A.; Chua, C. K.; Zhao, G.; Sofer, Z.; Pumera, M. *ACS Nano* **2012**, *6*, 8546−8551.
(17) Htun, H.; Dahlberg, J. E. *Science* **1989**, *243*, 1571−1576.
(18) Ren, J. S.; Chaires, J. B. *J. Am. Chem. Soc.* **2000**, *122*, 424−425.
(19) Plum, G. E.; Park, Y. W.; Singleton, S. F.; Dervan, P. B.; Breslauer, K. J. *Proc. Natl. Acad. Sci. U. S. A.* **1990**, *87*, 9436−9440.
(20) Feng, L. Y.; Li, X.; Peng, Y. H.; Geng, J.; Ren, J. S.; Qu, X. G. *Chem. Phys. Lett.* **2009**, *480*, 309−312.
(21) Jain, S. S.; Polak, M.; Hud, N. V. *Nucleic Acids Res.* **2003**, *31*, 4608−4615.
(22) Song, G. T.; Xing, F. F.; Ren, J. S.; Chaires, J. B.; Qu, X. G. *FEBS Lett.* **2005**, *579*, 5035−5039.
(23) Fan, X. J.; Liu, J.; Tang, H.; Jin, Y.; Wang, D. B. *Anal. Biochem.* **2000**, *287*, 95−101.
(24) Sklena, V.; Felgon, J. *Nature* **1990**, *345*, 836−838.
(25) Fuller, W.; Wilkins, W. H. *J. Mol. Biol.* **1965**, *12*, 60−76.
(26) Arcella, A.; Portella, G.; Ruiz, M.L.; Eritja, R.; Vilaseca, M.; Gabelica, V.; Orozco, M. *J. Am. Chem. Soc.* **2012**, *134*, 6596−6606.
(27) Feng, L. Y.; Chen, Y.; Ren, J. S.; Qu, X. G. *Biomaterials* **2011**, *32*, 2930−2937.
(28) Lubin, A. A.; Plaxco, K.W. *Acc. Chem. Res.* **2010**, *43*, 496−505.
(29) Li, X.; Peng, Y. H.; Ren, J. S.; Qu, X. G. *Biochemistry* **2006**, *45*, 13543−13550.
(30) Boon, E.M.; Barton, J. K. *Bioconjugate Chem.* **2003**, *14*, 1140−1147.
(31) Tanabe, K.; Lida, H.; Haruna, K. I.; Kamei, T.; Okamoto, A.; Nishimoto, S. I. *J. Am. Chem. Soc.* **2006**, *128*, 692−693.
(32) K'Owino, I. O.; Sadik, O. A. *Electroanalysis* **2005**, *17*, 2101−2113.
(33) Feng, L. Y.; Wu, L.; Wang, J. S.; Ren, J. S.; Miyoshi, D.; Sugimoto, N.; Qu, X. G. *Adv. Mater.* **2012**, *24*, 125−132.
(34) Hummers, W. S.; Offeman, O. S. *J. Am. Chem. Soc.* **1958**, *80*, 1339−1339.
(35) Ihara, T.; Ishii, T.; Araki, N.; Wilson, A. W.; Jyo, A. *J. Am. Chem. Soc.* **2009**, *131*, 3826−3827.
(36) Wang, J.; Musameh, M.; Lin, L. Y. *J. Am. Chem. Soc.* **2003**, *125*, 2408−2409.
(37) Ontko, A. C.; Armistead, P. M.; Kircus, S. R.; Thorp, H. H. *Inorg. Chem.* **1999**, *38*, 1842−1846.
(38) Dennany, L.; Forster, J. R.; White, B.; Smith, M.; Rusling, F. J. *J. Am. Chem. Soc.* **2004**, *126*, 8835−8841.
(39) Holmberg, R. C.; Thorp, H. H. *Inorg. Chem.* **2004**, *43*, 5080−5085.
(40) Kan, Y.; Schuster, G. B. *J. Am. Chem. Soc.* **1999**, *121*, 11607−11614.
(41) Nunez, M. E.; Noyes, K. T.; Gianolio, D. A.; Mclanghlin, L. W.; Barton, J. K. *Biochemistry* **2000**, *39*, 6190−6199.
(42) Radi, A. E.; Sanchez, J. L.; Baldrich, E.; O'Sullivan, C. K. *J. Am. Chem. Soc.* **2006**, *128*, 117−124.
(43) Weatherly, S. C.; Yang, I. V.; Thorp, H. H. *J. Am. Chem. Soc.* **2001**, *123*, 1236−1237.
(44) Oliveira-Brett, A. M.; Diculescu, V.; Piedade, J. A. P. *Biochemistry* **2002**, *55*, 61−62.
(45) Oliveira-Brett, A. M.; Piedade, J. A. P.; Serrano, S. H. P. *Electroanalysis* **2000**, *12*, 969−973.
(46) Richter, M. M. *Chem. Rev.* **2004**, *104*, 3003−3036.
(47) Suk, J.; Wu, Z.; Wang, L.; Bard, A. J. *J. Am. Chem. Soc.* **2011**, *133*, 14675−14685.
(48) Gerardi, R. D.; Barnett, N. W.; Lewis, S. W. *Anal. Chim. Acta* **1999**, *378*, 1−41.
(49) Rubinstein, I.; Bard, A. J. *J. Am. Chem. Soc.* **1981**, *103*, 512−516.
(50) Sistare, M.; Codden, S. J.; Heimlich, G.; Thorp, H. H. *J. Am. Chem. Soc.* **2000**, *122*, 4742−4749.
(51) Genereux, J.; Barton, J. K. *Chem. Rev.* **2010**, *110*, 1642−1662.
(52) Kan, Y.; Schuster, G. B. *J. Am. Chem. Soc.* **1999**, *121*, 10857−10864.